Characterization of β_3-adrenergic receptor: determination of pharmacophore and 3D QSAR model for β_3 adrenergic receptor agonism[★]

Philip Prathipati & Anil K. Saxena*
Division of Medicinal and Process Chemistry, Central Drug Research Institute, 226001, Lucknow, India

Summary

The β_3-adrenoreceptor (β_3-AR) has been shown to mediate various pharmacological and physiological effects such as lipolysis, thermogenesis, and intestinal smooth muscle relaxation. It also plays an important role in glucose homeostasis and energy balance. Molecular modeling studies were undertaken to develop predictive pharmacophoric hypothesis and 3D-QSAR model, which may explain variations in β_3-AR agonistic activity in terms of chemical features and physicochemical properties. The two softwares, CATALYST for pharmacophoric alignment and APEX-3D for 3D-QSAR modeling were used to establish the structure activity relationships for β_3-AR agonistic activity. Among the several statistically significant models, the selection of the best pharmacophore and 3D-QSAR model was based on its ability to estimate the activity of external test sets of similar and different structural types along with the reasonable consistency of the model with the limited information of the active site of β_3-AR. The final 3D-QSAR model was derived using the pharmacophoric alignments from the hypothesis which consisted of four chemical features: basic or positive ionizable feature on the nitrogen of the aryloxypropylamino group, two ring aromatic features corresponding to the phenyl ring of the phenoxide and the benzenesulphonamido groups and a hydrogen-bond donor (HBD) in the vicinity of the nitrogen atom of the benzenesulphonamido group with the most active molecule mapping in an energetically favorable extended conformation. This hypothesis was in agreement with the site directed mutagenesis studies on human β_3-AR and correlated well the observed and estimated activity both in, training and both the external test sets. It also mapped reasonably well to six β_3-AR agonists of different structural classes under clinical development and thus this hypothesis may have a universal applicability in providing a powerful template for virtual screening and also for designing new chemical entities (NCEs) as β_3-AR agonists.

Introduction

In recent years, the activation of human β_3-adrenergic receptor (β_3-AR) has attracted much attention [1–13] as a potential approach towards the treatment of obesity [14–20] and non-insulin dependent diabetes mellitus (NIDDM) [19–21], which is increasing at an alarming rate in western countries. The β_3-AR, which was initially (1980s) referred as atypical because of the characterization of only β_1- and β_2-AR at that time, also belongs to the seven transmembrane G-protein coupled receptor, present in white and brown adipose tissues [22], gastrointestinal tract [23], stomach [23] and some heart tissues [24]. It is implicated in the regulation of lipid metabolism. Stimulation of this receptor elevates cyclic AMP levels thereby stimulating lipolysis [25] and upregulation of adipose

specific genes. The increased expression of uncoupling protein (UCP-1), a brown adipose tissue specific mitochondrial protein, uncouples fatty acid oxidation from oxidative phosphorylation. The process increases heat production with a commensurate boost in energy consumption rendering β_3-AR agonists as potential antiobesity agents. Besides this, β_3-AR has also been shown to mediate various pharmacological and physiological effects such as intestinal smooth muscle relaxation [23], urinary bladder detrusor muscle relaxation [26–28] and is thought to play an important role in glucose homeostasis and energy balance in humans. Thus β_3-AR agonist therapy represents a novel approach to alter energy utilization and thus ameliorate obesity, NIDDM, intestinal hypermotility and urinary bladder dysfunction such as urinary frequency and incontinence.

The β_3-AR has been isolated and characterized only a decade ago and most of the information on the active site of β_3-AR has been gained from site directed mutagenesis and chimaric β_2-AR and β_3-AR studies [29] where only one amino acid residue 'Asp117' has been identified to be involved in the ligand binding. A homology model of β_3-AR, aligned upon bacteriorhodospin and β_2-AR, helped in assigning the specific amino acid residues to individual helices and in defining their particular roles with respect to structure and function of the receptor [19]. However as yet there is no X-ray structure of ligand β_3-AR complex except a few reports of an initial hypothesis on potential binding conformation [30, 31] and ligand receptor interactions [32, 33]. One of these papers describing the β_3-AR ligand interactions [33] deals mainly with β_1- and β_2-AR and makes casual remarks about β_3-AR. Although the other recent paper [33] which appeared during the course of this work describes the 3D model for β_3-AR complex with agonists and antagonists in terms of direct design where the β_3-AR ligands are shown to share most of the structural features common to β_1- and β_2-AR agonists. In this paper [33] the selectivity of β_3-AR agonists has been attributed predominantly to the interactions between the N-substituted carboxylate or sulphonamide group of the ligands with Arg315 (TM6). However it neither quantifies the results in terms of scores nor corroborates the results with the binding site information derived experimentally

from site directed mutagenesis studies. It also does not provide the plausible mechanisms for the agonist-induced activation. Hence it is prudent to identify possible pharmacophores from a series of aryloxypropanolamines with β_3-AR agonistic activities, to understand the molecular recognition in terms of physicochemical and structural requirements (pharmacophore) for potent and selective β_3-AR agonists. The concept of 'pharmacophore' imparts a qualitative source for providing the geometry of the active site. The recognition site or pharmacophore can be considered as a collection of functional groups exhibiting a three-dimensional array that mimics the geometry of the active site. Its identification through the study of three dimensional pattern of different substrate molecules in their energetically accessible conformations not only provide information about the active site but also provide essential structural requirements for the substrate to have good interactions at the receptor [34].

Among the several such approaches, one of the recent entries, which explores the conformational space efficiently and generates a chemical-feature based pharmacophoric hypothesis, is the CATALYST software [35–42]. Though these hypotheses represent the interactions at the active site, but have limitations in explaining the variations of activities within the required limits of residuals within one order of magnitude. This is because, the CATALYST is based on the assumption that an active molecule should map more features than an inactive molecule and so a molecule should be inactive because it either does not contain an important feature, or misses the feature, as it cannot be orientated correctly in space. The estimated activities by the CATALYST are based on the fit of the molecule to the features of the hypothesis and hence the estimations are more dependent on conformational/structural parameters than on physicochemical properties. As it is well accepted that the activities of a molecule depend both on the conformational (structural) and physicochemical properties (molecular and atomic), so in consequence improved predictive models may be obtained by creating hypothesis with variable feature weights or tolerances for obtaining electrostatic differentiation in CATALYST [35] or by the development of the 3D-QSAR models using APEX-3D [43], the later takes into consideration both conformational dependent structural parameters and physicochem-

ical properties (quantum chemical indexes, atomic point charges, β-populations, electron donor and acceptor indexes, atomic contributions to hydrophobicity, contributions to refractivity at various sites, centered on atoms of the ligand molecules) in terms of biophoric sites and secondary sites.

There are two basic approaches to develop 3D-QSAR models using APEX-3D, the black box approach and the gray box approach, the former approach involves building a model out of several hundred conformers generated for each molecule with exhaustive conformational analysis followed by clustering of the conformers to filter out those that do not add new information. Evidently this method is computationally very demanding and hence impractical for developing predictive models for virtual screening of an in-house built or a commercially available database. The latter approach is used when information such as X-ray structure of a ligand–receptor complex of some ligands, or an initial hypothesis on potential binding conformation and topography of potentially active sites (pharmacophoric hypothesis) based on experimental data and modeling experiments is available. This gray box approach is often used to derive 3D-QSAR models describing the binding of a ligand to a protein [44–49]. As there is no unique alignment solution, several binding modes based on various pharmacophoric alignments and global minimum energy conformations are explored through 3D-QSAR modeling. Herein the predictive ability of the 3D QSAR model for the test set helps in the selection of the best model, which may further be interpreted in terms of the ligand–receptor interactions [48]. Further the application of QSAR models for virtual screening places a special emphasis on statistical significance and predictive ability (validation) of these models as their most crucial characteristics. One of the most popular validation criteria, leave one out cross validated R2 (LOO Q2) as shown by the works of Wold, Golbraikh and Tropsha appears to be the necessary but not the sufficient condition for the model to have high predictive power [50–53]. Thus it appears that estimation of predictive power of the model is to test it on a sufficiently large collection of compounds, from an external test set approximately numbering about 1/3rd of the training set to establish a reliable QSAR model for virtual screening [53].

In view of the above, present studies were undertaken on β_3-AR agonists to obtain chemical feature based hypotheses and 3D-QSAR models which may explain variations, in activity across a set of molecules (both training and test sets) and may be useful in interpreting ligand–receptor interactions at the binding site and in virtual screening.

Methods

All molecular modeling studies were performed on Silicon Graphics O2 Irix 6.5 workstation running CATALYST software version 4.6 (Accelrys Inc.), APEX-3D software version 2.0 (Biosym).

β_3-AR agonists and experimental data

The structural series of molecules used in this study has been taken from the literature (Table 1) [11, 12] where activity range spans 4–5 orders of magnitude and also contains one of the most active β_3-AR agonist (molecule no. 41) reported till date. The β_3-AR agonistic activity has been described in an *in vitro* chinese hamster ovary cells expressing the cloned human β_3-AR to generate EC50 values. Out of the total set of 51 molecules of the two papers, a collection of 34 congeneric β_3-AR agonists was chosen as the training set using the picking rules for pharmacophore hypothesis generation as described in CATALYST [35, 54]. The 3D-QSAR models were developed on the pharmacophoric hypothesis alignments using APEX-3D [55–62] while the rest 17 compounds were used as an external test set to select the best model. To further validate the pharmacophoric hypothesis and 3D-QSAR models in terms of their predictive ability, another test set (testset-2) (Table 2) belonging to completely different structural class [13] was used.

Pharmacophore hypothesis generation and alignments

The pharmacophoric hypothesis generation and the pharmacophore-based alignments (i.e. conformational analysis, molecular fitting, etc) were performed using the basic modeling methodologies available within the CATALYST software. The implemented chemical features and the energy

minimization procedures viz. standard conjugate gradients minimization algorithm and a modified version of CHARMm [63] molecular mechanics force field which is proven to be equivalent to the semi-empirical method AM1, with no reports that it is not suitable for the present set of ligands [64] was used. Though the conformers could be generated either in a continuum solvent or *in vacuo* conditions, but in view of the non-availability of inclusion of solvation in conformation generation in CATALYST and its reported performance to reproduce the bioactive conformations of the protein-bound ligand in terms of efficiency and effectiveness in comparison to other softwares like Confort, Flo99, MacroModel (both *in vacuo* and in aqueous solution) and OMEGA [65], the CATALYST was used to generate the conformations for all molecules (both the training and test sets) using modified CharmM force field parameters and a constraint of 10 kcal mol^{-1} energy thresholds above the global energy minimum. CATALYST selects conformers using the poling algorithm [66, 67], which penalizes any newly generated conformer of it that is very close to any already found conformers. This method ensures maximum coverage in conformational space. All other parameters were set to their default settings. The different steps followed for pharmacophore hypothesis generation were based on the methodology implemented in CATALYST [35, 68] viz. (1) Conformational search as described above using the implemented force field and a poling function to ensure conformational diversity, (2) mapping of the chemical functionalities of each molecule and conformer, (3) identification of common chemical features based on the library of chemical descriptors [68] and valid spatial arrangement of the chemical features to generate pharmacophoric hypothesis, (4) geometric fit of each of the molecule based on the superimposition of equivalent functional groups without the modification of the geometry of the molecule (fast fit algorithm), and (5) analysis of the generated hypothesis.

Assessment of the quality of pharmacophore hypotheses

Cost function analysis
The evaluation of the quality of the generated pharmacophoric hypothesis was based on the cost

Table 1. Chemical structures and β_3-AR agonistic activities of the training and test set−1 (*) compounds.
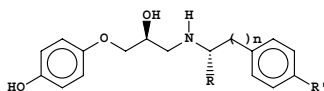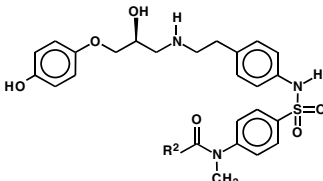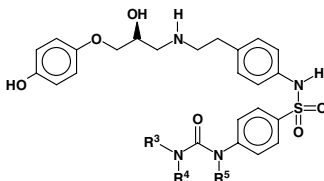

Comp. no.	n	R	R′	EC$_{50}$ nM	Comp. no.	R^2	EC$_{50}$ nM	Comp. no.	R^2	EC$_{50}$ nM	Comp. no.	R^3	R^4	R^5	EC$_{50}$ nM
1	2	Me	Ome	200	12	nPr	60	26*	(CH2)2Ph	5.9	40	Pr	H	H	1.1
2	2	H	Ome	600	13	nPent	4000	27*	3-Cl-Ph	15	41	Nhex	H	H	0.43
3	2	Me	OH	12	14	cHex	1500	28*	4-Cl-Ph	4.8	42	Chex	H	H	1.9
4	1	Me	Ome	1000	15	CH2Ph	39	29	Me	5	43	Nhex	H	Me	6.6
5	1	Me	OH	25	16	(CH2)3Ph	92	30	Et	1.4	44	Nhex	Me	Me	10
6	1	H	NH2	440	17	2-Cl–Ph	54	31	IsoPr	1.2	45*	Me	H	H	1.4
7	1	H	NHCOPh	27	18	4-Me-Ph	2.6	32	Ph	2.3	46*	Npent	H	H	5.2
8	1	H	NHSO$_2$ Ph	110	19	4-Ome-Ph	4.3	33	MeO	0.7	47*	Nhept	H	H	2.8
9	1	H	NHSO$_2$ Ph	6.3	20	3,4-(Cl)$_2$-Ph	58	34	EtO	1.1	48*	Oct	H	H	1
10*	1	H	OH	30	21	2-Naphthyl	5.4	35	BuO	1	49*	CH$_2$Opr	H	H	2.4
11*	1	H	NHCOPh	62	22	3-Quinolinyl	1.3	36*	IsoPr	2.6	50*	Ipr	H	H	1.2
					23	4-Br–Ph	0.77	37*	HexO	11	51*	Nhex	Me	H	2.1
					24	4-I–Ph	1.6	38*	Pr	6.8					
					25*	IsoPr	25	39*	Hex	1.4					

Table 2. Chemical structures and β_3AR agonistic activities of test set–2 compounds.

Comp number	X	EC$_{50}$ nM	Comp number	X	EC$_{50}$ nM	Comp number	X	EC$_{50}$ nM
52	1-(3-Hexyl-urea)	6.3	55	COMe	88	67	2-(4-Octyl-thiazole)	0.93
53	(4-octyl-thiazol-2-yl)-amine	0.8	56	COC$_6$H$_{13}$	7	68	2-(4-(3-Cyclopentyl-propyl)-thiazole)	3.2
54	Methyl-(4-octyl-thiazol-2-yl)-amine	5.5	57	COC$_8$H$_{17}$	55	69	2-(4-Hexyl-pyrimidine)	5.1
			58	CONHMe	6.9	70	2-(4-Octyl-pyrimidine)	2.4
			59	CONHC$_6$H$_{13}$	0.73	71	2-(6-Hexyl-pyridine)	1.2
			60	CON(Me)(C$_6$H$_{13}$)	47	72	2-(6-Octyl-pyridine)	1
			61	CON(Me)(C$_8$H$_{17}$)	18	73	2-(6-(3-Cyclopentyl-propyl)-pyridine)	1.7
			62	CON(Me)(CH$_2$CH$_2$Ph)	55	74	1-(3-Hexyl-benzene)	1.8
			63	3-(5-Hexyl-[1,2,4]oxadiazole)	13	75	1-(3-Octyl-benzene)	1.3
			64	3-(5-Octyl-[1,2,4]oxadiazole)	31	76	1-(3-(3-Cyclopentyl-propyl)-benzene)	5
			65	2-(4-Metyl-thiazole)	8.1	77	2-(5-Hexyl-pyridine)	1.6
			66	2-(4-Hexyl-thiazole)	0.9	78	2-Methyl-5-octyl-oxazole	3.7

functions reported by Sutter et al. [69] (represented in bits unit) and calculated by the CATALYST/hypogen module during hypothesis generation [35]. In brief, the cost (total cost) of a hypothesis is calculated by the following equation:

$$Cost = eE + wW + cC$$

where e, w, and c are the coefficients associated with the error (E), weight (W), and configuration (C) components, respectively.

Although the other two important cost calculations the 'fixed cost' and the 'null cost', the former represents the simplest model that perfectly fits the data and is calculated by the following equation:

$$Fixed\ cost = eE(x = 0) + wW(x = 0) + cC$$

where x is the deviation from the expected values of weight and error. The other null cost is the cost of a pharmacophore without any feature where the calculated activity data of each molecule in the training set is the average value of all activities. Therefore, the contribution from the weight or configuration component does not apply. The null cost is calculated from the following equation:

$$Null\ cost = eE(K_{est} = \kappa)$$

where K_{est} is the average scaled activity of the training set molecules. In CATALYST software the differences between the cost of the generated and the null hypothesis should be as large as possible, a value of 40–60 bits difference may indicate that there is only 75–90% chance of representing a true correlation in the data set used. The total cost of any hypothesis should be nearer to the value of the fixed cost for any meaningful model. The other two important output parameters are the configuration cost (also known as entropy cost) and the error cost. The former depends on the complexity of the pharmacophore hypothesis space. Any value higher than 17 may indicate that the correlation from any of the generated hypothesis is most likely due to chance, so either some attention has to be given in the selection of training set molecules or the entropy cost should be reduced by limiting the minimum and maximum features. The rms deviations represent the quality of the correlations between the estimated and the actual data.

Pharmacophore hypothesis generation with variable weight and tolerance options

Variable weight and variable tolerance hypothesis were generated by setting the respective parameters to a value of '1'. While the variable weight option generates hypothesis, which contain features with different weights, which have greater impact on activity than the others, the variable tolerance compensates for the deficiencies in the conformational coverage of unusually flexible compounds and optimizes the tolerances.

Table 3. Atomic indexes calculated in APEX-3D.

Index	Description
ACC_01	Electron acceptor reactivity of atoms
DON_01	Mean electron donor reactivity of atoms with lone pair
CHARGE	Point atomic charge in a.u.
HOMO	Squares of LCAO coefficients for highest occupied MO
LUMO	Squares of LCAO coefficients for lowest unoccupied MO
PI-POPUL	π-electron density on atoms
FORMAL_CHARGE	Formal charge on atoms
HYBRID_TYPE	Hybridization type of carbon atoms. The following coding is used: $1 - sp$, $2 - sp^2$, $3 - sp^3$
LP	Number of electron lone pairs on atoms
HYDROPHOBICITY	Atomic hydrophobicity increments
REFRACTIVITY	Atomic refractivity increments
PSEUDO	Dummy property. Equal to 1 for all atoms

Global minimum energy conformations: simulated annealing (Molecular Dynamics)

The molecular dynamics technique of simulated annealing was applied to identify the global minimum energy conformation following the general approach described in our previous papers [56]. In this procedure the optimized conformations of compound no. 41 (the most active compound) was randomized by setting random velocities and carrying out MD simulations at 0.1 ps at a temperature of $T = 1000$ K with a distance dependent dielectric constant *in vacuo* using the CVFF forcefield as implemented in insightII. The obtained average conformations of compound no. 41 by this calculation were used as starting point for another 5 ps of MD simulations at $T = 1000$ K. The purpose of high temperature was to explore conformational space extensively. An annealing procedure was subsequently applied to each average conformation obtained in high temperature simulations. The annealing was carried out, as slow cooling down of the structure from 1000 to 300 K. The last step of an annealing procedure was energy minimization. In this approach, a total of 75–150 ps of simulation time was obtained. The most active molecule in its global minimum energy conformation was edited in the builder module of insightII to obtain the

structures of all the other 50 (fifty) molecules and thus it may be assumed that the conformations of other molecules is limited in terms of torsion angles. These 3D structures were later optimized for their geometry using CVFF forcefield [70, 71] and the energy minimization was performed using the steepest descent, conjugate gradient, Newton–Raphsons algorithms in sequence followed by Quasi Newton Raphson (va09a) implemented in the discover module by using 0.001 kcal/mol. energy gradient convergence and maximum number of iteration set to 1000 and the molecular structures were exported for 3D QSAR model development by APEX-3D.

3D-QSAR model generation using APEX-3D

The APEX-3D methodology was applied following the general approach described in our previous papers [56–62]. The molecular structures, obtained either through pharmacophoric hypothesis alignments or conformations based on the global minimum energy conformation of the most active molecule, were stored in MDL format for computation of MOPAC version 6.0 based indices (MNDO Hamiltonian), such as atomic charge, β-population, electron donor and acceptor index, HOMO and LUMO coefficients and hydrophobicity and molar refractivity based on atomic

Table 4. Characteristics of 12 CATALYST derived hypotheses.

No	Hypothesis	Chemical features	Diff. in cost	Configuration	Correlation coefficient		
					Training set[a]	Test set – 1 (17 mol.)	Test set – 2 (27 mol.)
1	A	RA, HBD, PosI, RA (2009)	44	15.57	0.85	0.675	0.7733
2	A1	HBD, PosI, RA, RA (1299)	43.379	27.182	0.92	0.77	0.6797
3	A2	HBD, PosI, HBD, RA (3216)	35.341	27.182	0.88	0.48	0.6015
4	B	HBA, PosI, HBA, R. A (2020)	49	17.69	0.90	0.615	0.5822
5	B1	HBA, HBA, Pos. I, RA (1546)	34.892	29.298	0.88	0.76	0.5490
6	B2	HBA, Pos. I, RA, RA (3215)	35.214	29.298	0.90	0.614	0.4691
7	C	HBA, PosI, HBA, HYD (237759)	40	17.90	0.84	0.673	0.6473
8	C1	HBA, HYD, HYD, PosI (3705)	31.987	29.534	0.86	0.77	0.5793
9	C2	HBA, HYD, HYD, PosI (3217)	27.887	29.534	0.848	0.911	0.4082
10	D	HBD, PosI, HBD, HYD (237760)	42	15.60	0.84	0.633	0.5068
11	D1	HBD, HYD, HYD, PosI (6035)	35.344	27.161	0.87	0.81	0.5254
12	D2	HBD, HBD, HYD, PosI (3218)	29.823	27.161	0.849	0.795	0.5267

RA, Ring aromatic; HBD, Hydrogen bond donor; HBA, Hydrogen bond acceptor; PosI, Positive ionizable; HYD, Hydrophobic.
[a]The regression lines that correlate for each hypothesis the actual versus estimated values, as implemented within CATALYST, were used to select the models A–D.
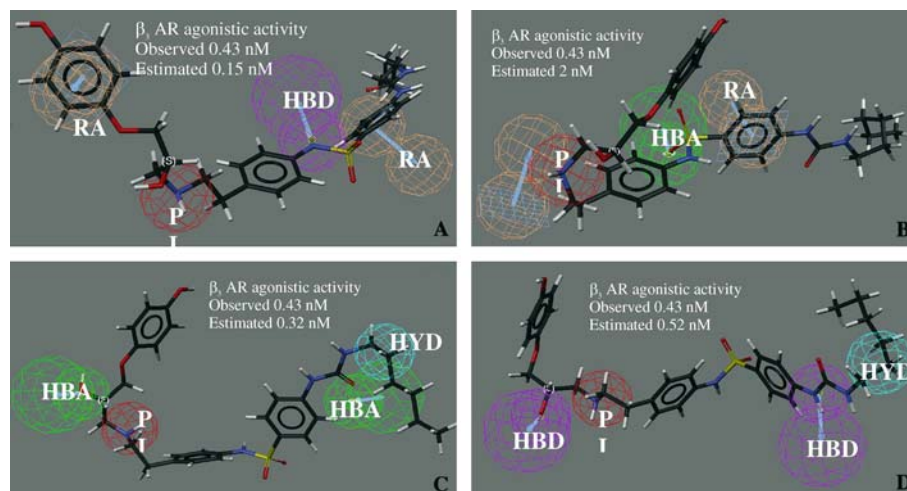
Figure 1. Mapping of the most active molecule (no. 41) to pharmacophoric hypotheses A, B, C and D which consist of a Positive Ionizable (PI), Hydrogen bond donor (HBD), Hydrogen bond acceptor (HBA), Hydrophobic (HYD) and Ring aromatic (RA).

contributions as shown in Table 3. The 3D-QSAR equations were derived with the site radius set at 0.90, site occupancy (minimum number of compounds, which must occupy a site before it can be included as a site) at 12, sensitivity at 1.0 and randomizations at 100. The biophoric sites and secondary sites combined to global properties (total hydrophobicity, total refractivity, and indicator) were used to obtain an equation to predict the pharmacological activity. The biophoric sites were set to charges, β-population, HOMO, LUMO, hydrogen acceptor, hydrogen donor, refractivity and hydrophobicity. The secondary sites were set to presence of hydrogen acceptor, hydrogen donor, heteroatom and ring and other parameters hydrophobic and steric to hydrophobicity and refractivity. (For more details, see the APEX-3D manual at http:// http://btcpxx. che.uni-bayreuth.de/COMPUTER/Software/MSI/ insight972/apex/2-Theory.doc.html(3201004)

Results and discussion

The purpose of the present investigation was to derive a predictive pharmacophoric hypotheses and 3D-QSAR model, which may explain the variation in activity among the molecules described in training and test set. Such model in addition of providing insights into β_3-AR-ligand interactions, may also be useful for virtual screening.

Among the initial run, the CATALYST software generated hypotheses which had configuration cost much above the acceptable limit of 17 and were also without the positive ionizable feature on the basic nitrogen, which is considered as an essential requirement for ligand–receptor interactions in case of adrenergic receptors including β_3-AR where site-directed mutagenesis studies, have shown Asp117 to be essential for binding of the ligand to the human β_3-AR [19, 29]. Hence three out of the total five surface accessible chemical functions viz. hydrogen bond donor (HBD), hydrogen bond acceptor (HBA), positive ionizable (PI), hydrophobic (HYD) and ring aromatic (RA) were taken at a time and all possible ten (10) combinations were used for hypothesis generation. The lowest cost hypothesis from each run was considered as the best and thus ten hypotheses were obtained. These hypotheses were evaluated and four hypotheses – A, B, C and D (Table 4) were identified on the basis of the following criteria, presence of a positive ionizable feature on the amine functionality, configuration cost (17, an over all cost difference between the current and null hypotheses (40) and with a good predictive ability (test set predictions) and are shown mapping to the most active compound (Figure 1). All these hypotheses had the positive ionizable group on the nitrogen of the propylamino group as one common pharmacophoric element to which all the β_3AR agonists have been found to map. The hypotheses A and B have ring aromatic groups
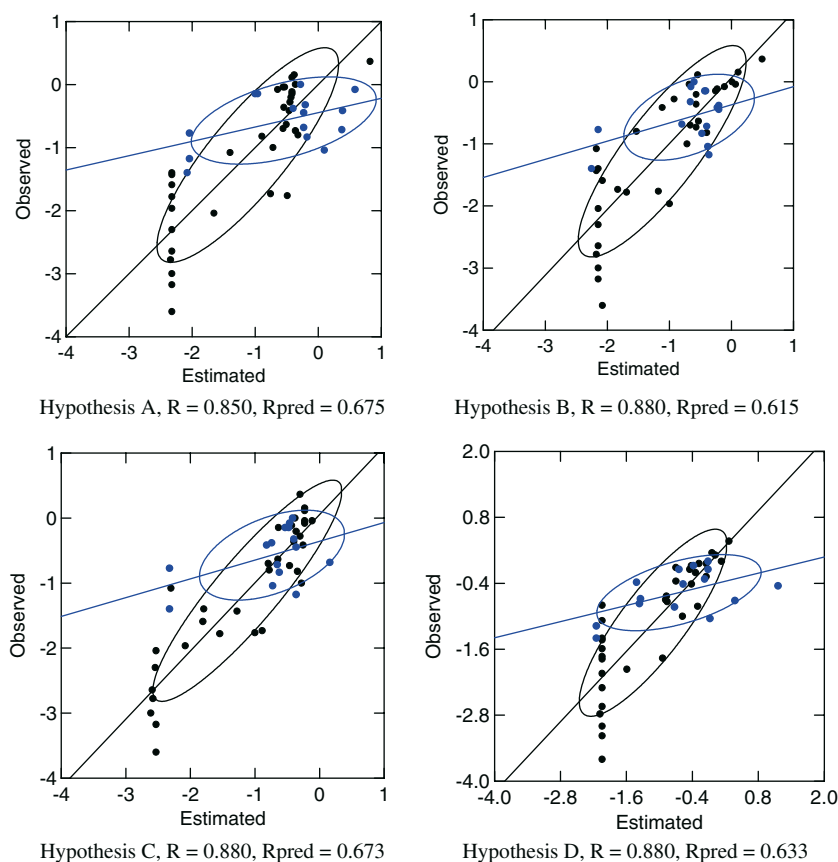
Figure 2. The plots of the observed versus estimated β_3AR agonistic activity from hypotheses (hypotheses A, B, C and D) for the training (•) and test (•) sets. The ellipse, with its regression line near and away from the origin represents the confidence ellipse of the estimations and predictions of the training and test set, respectively.

corresponding to the phenyl rings of the phenoxide and the benzenesulphonamido groups which are not mapped by all the molecules. The other two models C and D also have two common features, hydrogen bond donor and hydrophobic features in the vicinity of oxygen of ethanolamino group and the long aliphatic carbon chain of the

3-hexyl-ureido group, respectively. In addition to above, the hypothesis A and B also possess HBD and HBA feature in the vicinity of the nitrogen atom and oxygen atom of the bezenesulphoamide group, respectively, while the hypothesis C and D possess a HBA and HBD feature in the vicinity of Oxygen of CO group and N of the ureido group,
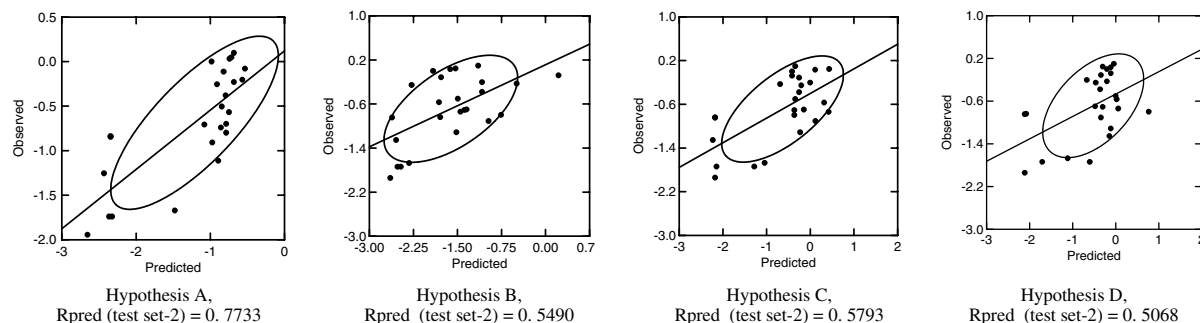

Figure 3. The plots of the observed versus estimated β_3AR agonistic activity by the standard hypotheses (A, B, C and D) for the test set-2.
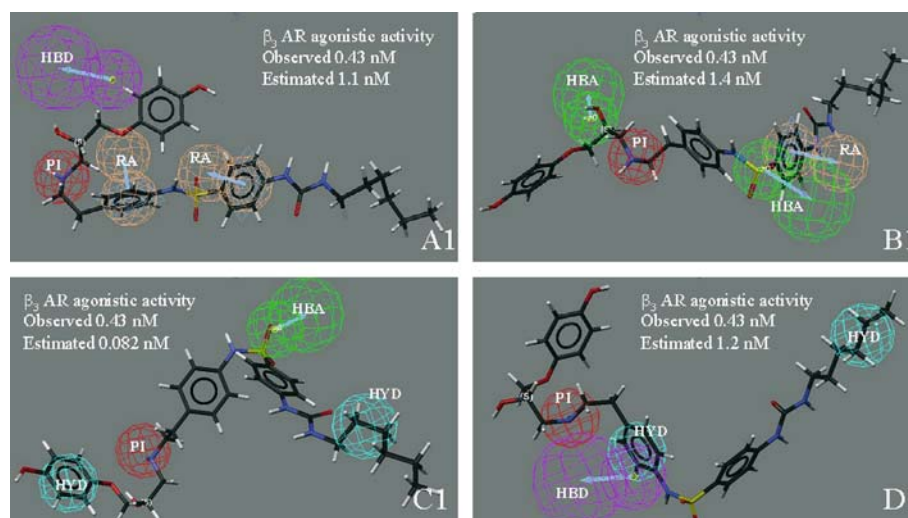
Figure 4. Mapping of the most active molecule (no. 41) to pharmacophoric hypotheses A1, B1, C1 and D1 which consist of a Positive Ionizable (PI), Hydrogen bond donor (HBD), Hydrogen bond acceptor (HBA), Hydrophobic (HYD) and Ring aromatic (RA).

respectively. The study of the inter-feature distances observed in these hypotheses (Figure 1) reveals that the long and flexible alkylamine chains in these β_3-AR agonists may exist both in the extended or stacked conformations and thus conforms with the previously published conformational analysis of β_3-AR agonists [30, 31].

The above hypotheses showed a good agreement between the observed and predicted activity of both the training and the test sets (Table 4). Although the results were statistically significant in terms of cost, but had limitations in explaining the

variations of activities within the required limits of residuals with many molecules estimated to have same activity (Figures 2 and 3). This limitation could be due to the fact that CATALYST standard considers only structural parameters for estimating the activities of molecules.

One way of considering both the structural/conformational and electrostatic parameters for the differentiation of activities is the use of variable weight and tolerance options in CATALYST predictive pharmacophoric hypothesis generator. Since the hypotheses without positive ionizable
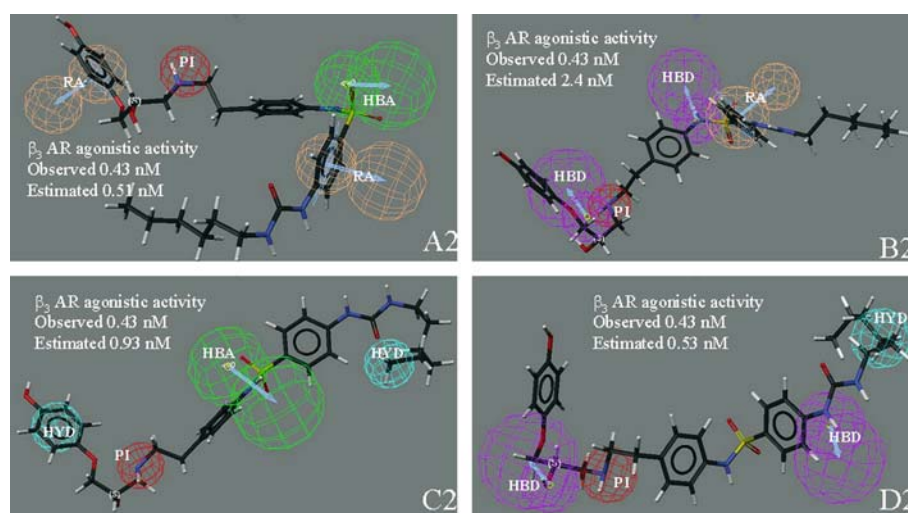

Figure 5. Mapping of the most active molecule (no. 41) to pharmacophoric hypotheses A2, B2, C2 and D2 which consist of a Positive Ionizable (PI), Hydrogen bond donor (HBD), Hydrogen bond acceptor (HBA), Hydrophobic (HYD) and Ring aromatic (RA).

Table 5. Statistical details of the 3D QSAR models developed using APEX-3D.

Model number	I	II	III
Number of compounds	34	34	34
Number of variables	4	5	4
$F_{(4, 28)}$	19.712	23.254	22.527
R, coefficient of correlation	0.858	0.907	0.880
R-square	0.735	0.823	0.775
Adjusted R-square	0.694	0.771	0.723
RMSA	0.600	0.519	0.571
RMSP	0.644	0.629	0.757
Probability of chance correlation	0.020	0.000	0.010
Match	0.21	0.68	0.62
Test set predictions	0.840		0.806

RMSA, Root mean squared error of activity approximation; RMSP, Root mean squared error of activity prediction calculated using leave-one out cross validation.
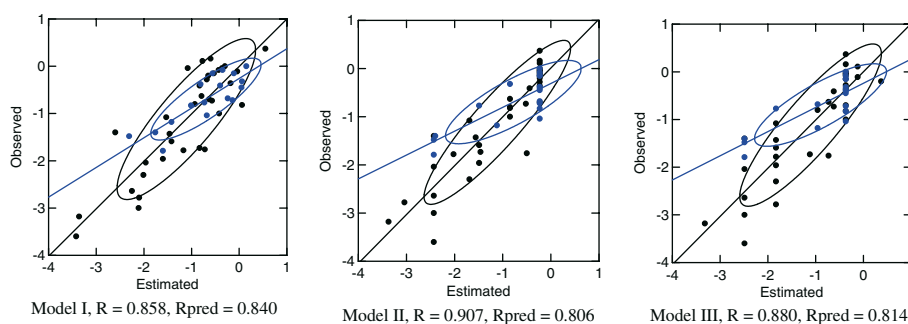

Model I, R = 0.858, Rpred = 0.840 Model II, R = 0.907, Rpred = 0.806 Model III, R = 0.880, Rpred = 0.814

Figure 6. The plots of the observed versus estimated β_3AR agonistic activity by APEX-3D models (I–III) for the training (•) and test (•) set. The ellipse, with its regression line near and away from the origin represents the confidence ellipse of the estimations and predictions of the training and test set, respectively.

feature and hydrogen bonding features are not desirable as discussed above, only the four hypotheses out of the ten possible hypotheses were considered. The optimized variable weight (A1-D1) and variable tolerance (A2-D2) hypotheses improved the predictive ability of the training set (Table 4) and test set-1 which contains molecules with similar structural classes, (Table 4) however the predictive ability for the external test set-2 containing molecules of a different structural class deteriorated (Table 4). Moreover these hypotheses with configurational cost (>27) may not be acceptable due to the violation of acceptable limits for configurational cost (<18) of these hypotheses (Table 4), which is indicative of the poor statistical significance of these optimized hypotheses. Unlike the expected similar feature types and positions in these optimized hypotheses as compared to the standard hypotheses (A-D) [69], these variable weight (Figure 4) and tolerance

(Figure 5) hypotheses produced pharmacophore features with different positions. Thus it appears that variable weight and tolerance hypotheses improve the correlation of the observed versus calculated activities of the training set and the observed versus predicted activities for a test set of similar molecules (test set-1), but they may not show the similar predictivity for the molecules of different structural classes (test set-2) (Table 4) and may have low statistical significance.

In order to develop improved models, the conformers obtained by mapping of the molecules to these four standard hypotheses were exported for 3D-QSAR model development. In addition to these four standard pharmacophoric (A, B, C and D) hypothesis-aligned conformers, the conformers based on the global minimum energy conformation of the most active compound were used and so in all 5 APEX-3D tasks were run to develop 3D QSAR models.
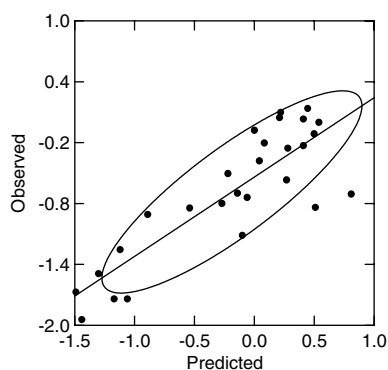
Figure 7. The plot of the observed versus estimated β_3AR agonistic activity by APEX-3D derived model I for the test set-2.

Out of the several thousands of 3D-QSAR models generated using APEX-3D, only models containing all the compounds with meaningful biophores (containing nitrogen as an element of the pharmacophoric/biophoric model), with good statistical parameters for the training set ($r > 0.85$, Chance < 0.1, RMSA < 0.8, RMSP < 1.0) and exhibiting good predictive ability against a test set ($r > 0.8$) were chosen.

Three such models (1–III) are described with their statistical details in Table 5 and the observed verses predicted activities for both test and training sets in Figure 6. The model I was derived using alignments obtained by pharmacophoric hypothesis A and model II and III were obtained from the conformations based on the global minimum energy conformation of the most active compound.

Although the above models, II and III, mapped all the molecules of the training and test sets and exhibited good statistics for both training ($r = 0.907$ and 0.886) and test sets ($r = 0.806$ and 0.814), but
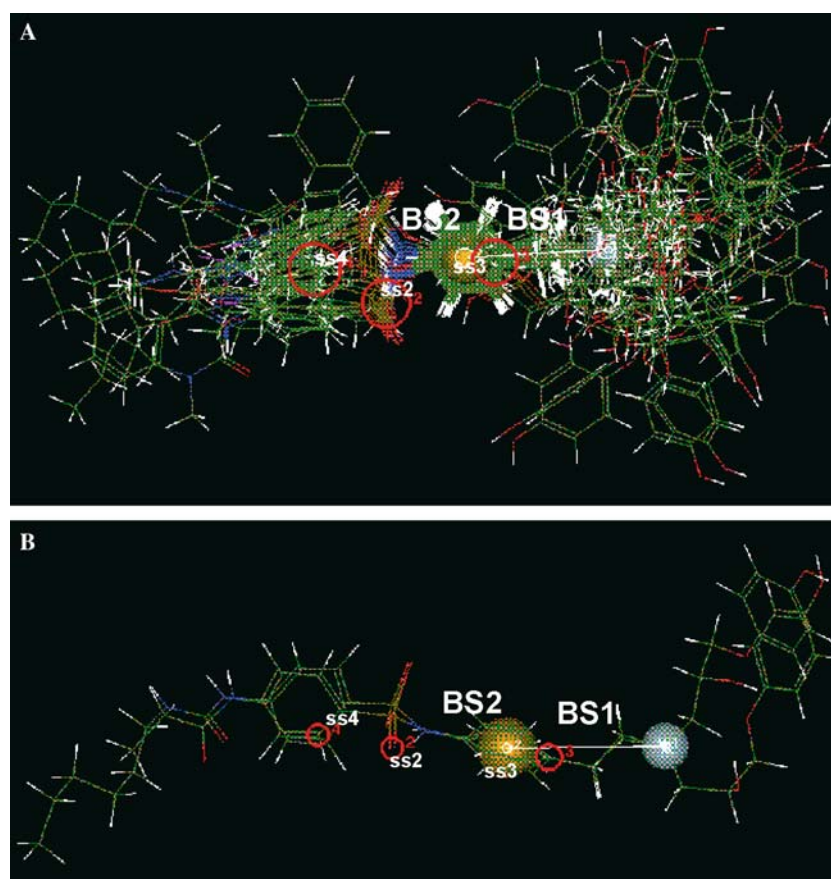

Figure 8. The 3D QSAR model derived using APEX-3D. The biophoric/pharmacophoric sites are represented by the solid spheres and the secondary sites are represented by hollow red circles. (a) Depicts the superimposition of all compounds of the training set according to the biophore/pharmacophore for model I and (b) depicts the superimposition of compounds 41 (the most active molecule) and 45, on the biophoric and secondary sites of model I.

Table 6. The β_3-AR agonistic activities and the global, biophoric and secondary site properties of compounds used in APEX-3D derived model 1.

| Comp. No.	−log EC$_{50}$ nM			Secondary sites			
	Observed	Estimated	Predicted	ss1*	ss2*	ss3*	ss4*
1	−2.30	−2.01	−1.97	2.18	–	–	–
2	−2.78	−2.10	−2.02	2.08	–	–	–
3	−1.08	−1.53	−1.61	2.07	–	0.58	–
4	−3.00	−2.11	−2	2.08	–	–	–
5	−1.40	−2.60	−2.92	1.97	–	−0.39	–
6	−2.64	−2.25	−2.19	1.94	–	–	–
7	−1.14	−1.46	−1.51	2.14	–	0.58	–
8	−2.04	−1.96	−1.96	2.22	–	–	–
9	−0.80	−0.93	−0.95	2.66	0.59	–	0.00
12	−1.78	−1.17	−1.11	2.43	–	0.58	–
13	−3.60	−3.42	−3.23	2.63	0.59	–	−2.46
14	−3.18	−3.36	−3.55	2.69	0.59	–	−2.46
15	−1.59	−1.42	−1.4	2.77	–	–	–
16	−1.96	−1.60	−1.5	2.98	–	−0.39	–
17	−1.73	−0.83	−0.77	2.77	–	0.58	–
18	−0.41	−0.83	−0.86	2.77	–	0.58	0.00
19	−0.63	−0.79	−0.81	2.80	0.59	–	–
20	−1.76	−0.72	−0.56	2.87	0.59	–	–
21	−0.73	−0.57	−0.56	3.03	–	0.58	–
22	−0.11	−0.04	−0.02	2.97	0.59	0.58	0.00
23	0.11	−0.77	−0.84	2.83	–	0.58	–
24	−0.20	−0.65	−0.72	2.94	0.59	–	0.00
29	−0.70	−0.63	−0.63	2.97	–	0.58	0.00
30	−0.15	−0.53	−0.56	3.07	–	0.58	0.00
31	−0.08	−0.43	−0.47	3.17	–	0.58	–
32	−0.36	−0.18	−0.15	3.41	0.59	0.00	–
33	0.16	−0.60	−0.71	2.99	0.59	–	–
34	−0.04	−1.08	−1.2	3.10	–	–	0.00
35	0.00	−0.30	−0.33	3.30	–	0.58	–
40	−0.04	−0.36	−0.39	3.24	–	0.58	–
41	0.37	0.55	0.59	3.55	0.59	0.58	–
42	−0.28	−0.68	−0.76	3.50	–	–	–
43	−0.82	0.06	0.22	3.66	–	0.58	0.00
44	−1.00	−0.42	−0.23	3.77	–	–	–

*ss – secondary site.
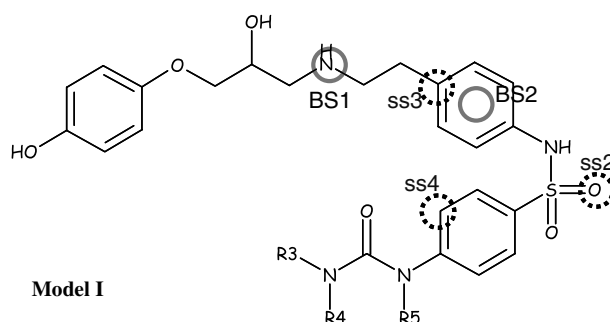
Model I

Figure 9. Schematic representation of the best model APEX-3D derived model I: the thick lined circles represent the biophoric sites (BS) and the broken lined circles represent the secondary sites (ss).

both the models predicted several molecules to have the same activity. Hence these models were also not desirable and so model I was chosen as the best 3D-QSAR model that could explain the variation between the observed and calculated β_3-AR agonistic activity for the training ($R = 0.858$) and the test set-1 ($R = 0.840$) (Figure 6). This model also predicted well the test set-2 with different structural type ($R = 0.855$) (Figure 7).

This model I derived from pharmacophoric hypothesis 'A' has two biophoric sites: one electron rich nitrogen atom of the aryloxypropanolamino group capable of donating electrons as biophoric site (BS1) and the second being center of the 6π-electron cloud of the phenyl ring of phenyl ethylamine part (BS2).

These biophoric sites (pharmacophore) present in each compound of the training set are important for β_3-AR agonistic activity and depend not only on the physicochemical properties of the biophoric centers corresponding to sites BS1 (π-population: 0.105 ± 0.01 [atomic units, au], charge_het: -0.32 ± 0.04 [au] and Don_01: 7.346 ± 1.24 [au] and BS2

(Cycle size: 6 ± 0[au] and π-population: 6 ± 0 [au], but also on their spatial disposition, the mean distances in angstroms unit between the biophoric descriptor centers being BS1-BS2 (5.391 ± 1.562) (Figure 8a and b).

In addition to the identification of the two common key structural features described above as biophoric sites for all molecules, three-dimensional quantitative structure–activity relationship (3D-QSAR) in terms of β_3-AR agonistic activity ($-\log EC_{50}$) as dependent parameter and physicochemical properties of different biophoric and secondary sites as independent parameter was derived using this pharmacophore as a template for superimposition. The *in vitro* β_3-AR agonistic activity was related to one global property and three secondary site (ss) parameters (Table 6) viz. Positively contributing parameters include refractivity as a global property, presence of hydrogen acceptor in the vicinity of oxygen of the sulfonamido group (ss2), hydrophobicity in the vicinity of BS2 (ss3) and hydrophobicity in the vicinity of phenyl ring of benzene
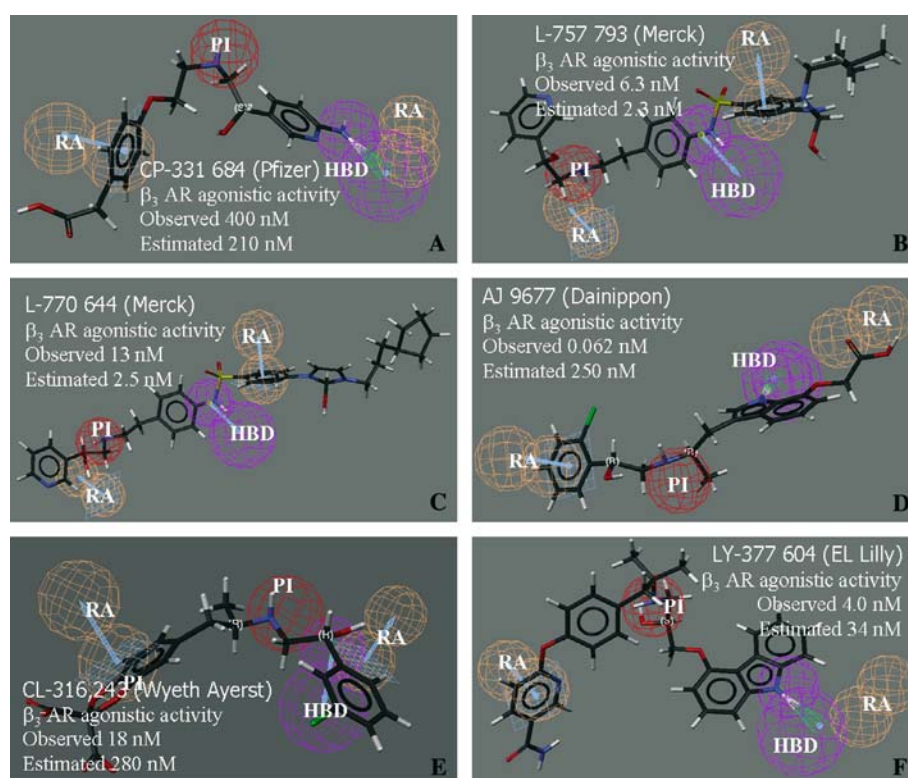

Figure 10. Mapping of six of the β_3AR agonists currently under development to hypothesis 'A' which consist of a Positive Ionizable (PI), Hydrogen bond donor (HBD), Hydrogen bond acceptor (HBA), Hydrophobic (HYD) and Ring aromatic (RA).

Table 7. Experimental and predicted activities with conformational energies of various β_3-AR agonists under clinical development.

Molecule	β_3-AR agonistic activity (EC$_{50}$ nM)		Conformational energy
	Experimental	Predicted[a]	
CL-316, 243	18	210	8.3470
L-770 644	13	2.5	2.5
L-757 793	6.3	2.3	5.90132
AJ 9677	0.062	250	16.7231
CP-331 684	400	280	6.67584
LY-377 604	4.0	34	8.26672

[a]Predicted activity values from hypothesis 'A'.

sulphonamide group (ss4) (Equation 1) [Table 6, Figures 8 and 9].

$$
\begin{aligned}
-\log(EC50) = {} & 0.022(\pm 0.005) \\
& (\textit{Total refractivity as global} \\
& \textit{property}) + 0.595(\pm 0.260) \\
& (\textit{Hydrogen acceptor at ss}2) \\
& + 3.891 \pm 1.340) \ (\textit{Hydrophobicity} \\
& \textit{at ss}3) + 4.919((0.963) \\
& (\textit{hydrophobicity at ss}4) \\
& - 4.184
\end{aligned} \tag{1}
$$

[$N = 34$, $R = 0.856$, RMSE $= 0.600$, RMSEP $= 0.64$, $F(4, 29) = 19.712$, Rpred $= 0.840$].

A comparison of this model with the pharmacophoric hypothesis 'A' derived by CATALYST suggests that out of the two biophoric sites BS1 and BS2, the site BS1 corresponds to the positive ionizable feature of hypothesis 'A', ss4 corresponds to the ring aromatic feature of hypothesis 'A' adjacent to the phenyl ring of the benzene sulphonamido group, while the ss3 corresponds to the hydrogen bonding feature of hypothesis A in the vicinity of sulphonamido group. The difference between the two lies in respect of the ring aromatic feature for the phenoxide ring in hypothesis 'A' and the benzene ring of phenyl ethylamino group in model I which may be due to the parameterization in terms of occupancy and site radius in APEX-3D. Further the model I is similar to the variable weight hypothesis 'A1' in terms of correspondence between BS1, BS2, ss2 and ss4 with PI, N-substituted RA, HBD and S-substituted RA, respectively.

Further to examine the validity of the pharmacophoric hypothesis 'A' against six of the β_3-AR agonists currently under development [72] viz. CL-316, 243 (Wyeth Ayerst) [73], L-770, 664

(Merck)[74], L-757 793 (Merck) [75], AJ 9677 (Dainippon) [76], CP-331 684 (Pfizer) [77] and LY-377 604 (Eli Lilly) [78] were mapped. These molecules map in a reasonable conformation to the above pharmacophoric hypothesis 'A' in varying degrees (Figure 10). All the molecules map to positive ionizable, the hydrogen bond donor and one of the ring aromatic features viz. the compounds CP-331 684, AJ 9677 and LY-377 604 to one of the ring aromatic feature while the other three molecules map to the other ring aromatic feature. A reasonable correlation ($R = 0.7$) was observed between the predicted and experimental activities in four of these molecules viz. CP-331 684, L-770, 664, L-757 793 and LY-377 604 (Table 7). Among the other two molecules viz. AJ 9677 and CL-316, 243, the former maps very well to two of the features RA and HBD and slightly misses the PI feature while the later maps well the RA and PI while completely misses the HBD feature as compared to the four other molecules. This may be the reason for their relatively poorer predictivity, nevertheless they do map to the hypothesis.

A comparison of this pharmacophoric hypothesis 'A' and the corresponding 3D-QSAR model with the recent the 'de novo' β_3-AR model of Furse and Lybrand [32] reveals that the aromatic ring (corresponding to the ring aromatic feature of hypothesis A) of the aryloxypropolamine corresponds to the aryl ring of adrenaline which interacts with Phe309 (TM6). The electron rich center (BS1) of the model I and the positive ionizable feature of hypothesis 'A' on the nitrogen of the aryloxypropanolamine corresponds to the nitrogen atom of the adrenaline, which is implicated in ionic salt–bridge interactions with Asp117 (TM3). As neither the pharmacophoric hypothesis

nor the 3D-QSAR model has any chemical feature nor sites corresponding to the hydroxyl functionality of the aryloxypropanolamine group, the validity of the hydroxyl-Asn312 (TM6) interactions in adrenaline β_3-AR complex as suggested by Furse and Lybrand is questionable. This is also supported from earlier reports [80], where dopamine a natural neurotransmitter without the beta-hydroxyl group, has been shown to selectively activate the β_3-AR and to a small extent the β_1-AR and the β_2-AR. Further several other ligands exhibit β_3-AR agonistic activity without the hydroxyl moiety like the tetrahydroisoquinolines [6]. Since the aryloxypropolamines class of molecules exhibit antagonistic activity with respect to both β_1- and β_2-AR, they could be possibly binding to β_3-AR without involving the hydroxyl-Asn312 interactions (the corresponding residue of Asn293 in β_2-AR). This was also confirmed by the site directed mutagenesis study where the N312A mutant of β_3-AR showed no variation in the binding parameters and effect parameters (either IA or EC_{50}) [29]. Finally in this model most of the pharmacophoric features, biophoric sites and secondary sites are on the N-substituted side chain of the aryloxypropanolamino group, particularly the hydrogen bonding site in the vicinity of oxygen of the sulphonamide group which aptly corroborates with the recent β_3-AR model of Furse and Lybrand where the major region for the selectivity and enhanced activity of the β_3-AR agonists has been assigned to the bulky side chains of aryloxypropanolamines with hydrogen bonding substituents like carboxylate or sulphonamide group [32, 79].

Conclusion

The present work has been focused on the development of predictive pharmacophoric hypothesis and 3D-QSAR model to elucidate the 3D structural and physicochemical requirements for the β_3-adrenoreceptor agonists. The selection of best pharmacophore and 3D-QSAR model was based on its ability to estimate the activity of an external test sets of both similar and different structural types and its reasonable consistency with the limited information on the active site of the β_3-AR. The 3D-QSAR model which demonstrated the best predictive ability against the test sets and also a good fit for the training set was derived from the pharmacophoric alignments of hypothesis 'A' which consisted of four chemical features: basic or positive ionizable feature on the nitrogen of the aryloxypropylamino group, two ring aromatic features corresponding to the phenyl ring of the phenoxide and the benzenesulphonamido groups and a hydrogen-bond donor in the vicinity of in the nitrogen atom of the bezenesulphonamide group with the most active molecule mapping in an energetically favorable extended conformation. This model not only explains the variation in activity among the training set molecules but also exhibits good test set predictions (external predictivity), which makes the QSAR study a significant one. The model also is in agreement with the site directed mutagenesis studies carried out on the human β_3-AR, where the ionic–salt bridge interactions between amine-Asp117 (TM3) have been implicated in agonistic binding, while the other hydrogen bonding interactions between hydroxyl-Asn312 (TM6) do not have significant influence on the binding affinity. Although this model explains the variation in the activity of the external test sets as well as maps reasonably well to six β_3-AR agonists of different structural classes under clinical development and thus may have a universal applicability in providing a powerful template for virtual screening and also for designing new chemical entities (NCEs) as β_3-AR agonists. However efforts are being made to further elucidate the role of other pharmacophoric and secondary site features important for binding and agonistic activation of β_3-AR by probing the bovine rhodposin based homology model of activated β_3-AR with the above pharmacophore.

Acknowledgements

References

1. Mathvink, R.J., Tolman, J.S., Chitty, D., Candelore, M.R., Cascieri, M.A., Colwell, L.F. Jr., Deng, L., Feeney, W.P., Forrest, M.J., Hom, G.J., MacIntyre,

D.E., Miller, R.R., Stearns, R.A., Tota, L., Wyvratt, M.J., Fisher, M.H. and Weber, , J. Med. Chem., 43 (2000) 3832.

2. He, Y., Nikulin, V.I., Vansal, S.S., Feller, D.R. and Miller, D.D., J. Med. Chem., 43 (2000) 591.

3. Zheng, W., Nikulin, V.I., Konkar, A.A., Vansal, S.S., Shams, G., Feller, D.R. and Miller, D.D., J. Med. Chem., 42 (1999) 2287.

4. Hu, B., Ellingboe, J., Han, S., Largis, E., Mulvey, R., Oliphant, A. and Sum Tillett, F.W.J., J. Med. Chem., 44 (2001) 1456.

5. Uehling, D.E., Donaldson, K.H., Deaton, D.N., Hyman, C.E., Sugg, E.E., Barrett, D.G., Hughes, R.G., Reitter, B., Adkison, K.K., Lancaster, M.E., Lee, F., Hart, R., Paulik, M.A., Sherman, B.W., True, T. and Cowan, C., J. Med. Chem., 45 (2002) 567.

6. Brockunier, L.L., Candelore, M.R., Cascieri, M.A., Liu, Y., Tota, L., Wyvratt, M.J., Fisher, M.H., Weber, A.E. and Parmee, E.R., Bioorg. Med. Chem. Lett., 11 (2001) 379.

7. Ok, H.O., Reigle, L.B., Candelore, M.R., Cascieri, M.A., Colwell, L.F., Deng, L., Feeney, W.P., Forrest, M.J., Hom, G.J., MacIntyre, D.E., Strader, C.D., Tota, L., Wang, P., Wyvratt, M.J., Fisher, M.H. and Weber, A.E., Bioorg. Med. Chem. Lett., 10 (2000) 1531.

8. Feng, D.D., Biftu, T., Candelore, M.R., Cascieri, M.A., Colwell, L.F. Jr., Deng, L., Feeney, W.P., Forrest, M.J., Hom, G.J., MacIntyre, D.E., Miller, R.R., Stearns, R.A., Strader, C.D., Tota, L., Wyvratt, M.J., Fisher, M.H. and Weber, A.E., Bioorg. Med. Chem. Lett., 10 (2000) 1427.

9. Parmee, E.R., Brockunier, L.L., He, J., Singh, S.B., Candelore, M.R., Cascieri, M.A., Deng, L., Liu, Y., Tota, L., Wyvratt, M.J, Fisher, M.H. and Weber, A.E., Bioorg. Med. Chem. Lett., 10 (2000) 2283.

10. Steffan, R.J., Ashwell, M.A., Solvibile, W.R., Matelan, E., Largis, E., Han, S., Tillet, J. and Mulvey, R., Bioorg. Med. Chem. Lett., 12 (2002) 2957.

11. Weber, A.E., Mathvink, R.J., Perkins, L., Hutchins, J.E., Candelore, M.R., Tota, L., Strader, C.D., Wyvratt, M.J. and Fisher, M.H., Bioorg. Med. Chem. Lett., 8 (1998) 1110.

12. Parmee, E.R., Ok, H.O., Candelore, M.R., Tota, L., Deng, L., Stander, C.D., Wyvaratt, M.J., Fisher, M.H. and Weber, A.E., Bioorg. Med. Chem. Lett., 8 (1998) 1107.

13. Mathvink, R.J., Barritta, A.M., Candelore, M.R., Cascieri, M.A., Deng, L., Tota, L., Strader, C.D., Wyvratt, M.J., Fisher, M.H. and Weber, A.E., Bioorg. Med Chem Lett., 9 (1999) 1869.

14. (a) Steffan, R.J., Ashwell, M.A., Solvibile, W.R., Matelan, E., Largis, E., Han, S., Tillet, J. and Mulvey, R., Bioorg. Med. Chem. Lett., 12 (2002) 2957. (b) Berkowitz, D.E., Nardone, N.A., Smiley, R.M., Price, D.T., Kreutter, D.K. and Fremeau, R.T., Eur. J. Pharmacol., 289 (1995) 223.

15. Clement, K., Vaisse, C., Mannings, B.S.J., Basdevant, A., Guy-Grand, B. and Ruis, J., N. Engl. J. Med., 333 (1995) 352.

16. Himms-Hagen, J., In Obesity, V., Johrporp, P. and Bordoll, B.N., Eds., Lippin Cott, Philadelphia, 1992, 15, 2.

17. Arch, J.R.S., Aimsworth, A.T., Cawthorme, M.A., Piercy, V., Sennitt, M.V., Thody, V.A., Wilson, C. and Wilson, S., Nature, 309 (1984) 163.

18. Dow, R.L., Exp. Opin. Invest. Drugs., 6 (1997) 1811.

19. Strosberg, A.D., Trends Pharmacol. Sci., 18 (1997) 449.

20. Arch, J.R.S. and Wilson, S., Int. J. Obes., 20 (1996) 191.

21. Sakane, N., Yoshida, T., Yoshioka, K., Nakamura, Y., Umekawa, T., Kogure, A., Takakura, Y. and Kondo, M., Diabetologia., 41 (1998) 1533.

22. Ghorbani, M., Claus, T.H. and Himms-Hagen, J., Biochem. Pharmacol., 54 (1997) 21.

23. Anthony, A., Schepelmann, S., Guillaume, J.L., Strosberg, A.D., Dhillon, A.P., Pounder, R.E. and Wakefield, A.J., Aliment Pharmacol. Ther., 12 (1998) 519.

24. Gauthier, C., Tavernier, G., Charpentier, F., Langin, D. and Le Marec, H., J. Clin. Invest., 98 (1996) 556.

25. Russell, S.T., Hirai, K. and Tisdale, M.J., Br. J. Cancer., 86 (2002) 424.

26. Igawa, Y., Yamazaki, Y., Takeda, H., Hayakawa, K., Akahane, M., Ajisawa, Y., Yoneyama, T., Nishizawa, O. and Andersson, K.E, Br. J. Pharmacol., 126 (1999) 819.

27. Igawa, Y., Yamazaki, Y., Takeda, H., Hayakawa, K., Akahane, M., Ajisawa, Y., Yoneyama, T., Nishizawa, O. and Andersson, K.E., J. Urol., 165 (2001) 240.

28. Tanaka, N., Tamai, T., Mukaiyama, H., Hirabayashi, A., Muranaka, H., Akahane, S., Miyata, H. and Akahane, M., J. Med. Chem., 44 (2001) 1436.

29. Gros, J., Manning, B.S., Pietri-Rouxel, F., Guillaume, J.L., Drumare, M.F. and Strosberg, A.D., Eur. J. Biochem., 251 (1998) 590.

30. Amici, M.D., Micheli, C.D., Kassi, L., Carrea, G., Ottolina, G. and Colombo, G., Tetrahedron, 9 (2001) 1849.

31. Guan, X.M., Amend, A. and Strader, C.D., Mol. Pharmacol., 48 (1995) 492.

32. Furse, K.E. and Lybrand, T.P., J. Med. Chem., 46 (2003) 4450.

33. Nagatomo, T. and Koike, K., Life Sci., 66 (2000) 2419.

34. Patel, Y., Gillet, V.J., Bravi, G. and Leach, A.R., J. Comput. Aided Mol. Des., 16 (2002) 653.

35. CATALYST Version 4.6, Accerlys, San Diego, CA.

36. Debnath, A.K., J. Med. Chem., 46 (2003) 4501.

37. Clement, O.O., Freeman, C.M., Hartmann, R.W., Handratta, V.D., Vasaitis, T.S., Brodie, A.M. and Njar, V.C., J. Med. Chem., 46 (2003) 2345.

38. Barreca, M.L., Gitto, R., Quartarone, S., De Luca, L., De Sarro, G. and Chimirri, A., J. Chem. Inf. Comput. Sci., 43 (2003) 651.

39. Palomer, A., Cabre, F., Pascual, J., Campos, J., Trujillo, M.A., Entrena, A., Gallo, M.A., Garcia, L. and Mauleon Espinosa, D., J. Med. Chem., 45 (2002) 1402.

40. Debnath, A.K., J. Med. Chem., 45 (2002) 41.

41. Kraft, P., Bajgrowicz, J.A., Denis, C. and Frater, G., Angew. Chem. Int. Ed., 39 (2000) 2980.

42. http://www.accelrys.com/references/rdd_pub.html(CATALYST.

43. Golender, V.E. and Rozenblit, A.B. (1983) Logical and Combinatorial Algorithms in Drug Design, Research Studies Press: Letchworth, UK, Golender, V.E., Vorpagel E.R. In: 3D QSAR in Drug Design: Theory, Methods and Applications, Kubinyi H. (Ed), ESCOM, Leiden, 1993, 137–149.

44. Martin, Y.C., Bures, M.G., Danaher, E.A., DeLazzer, J. and Lico Pavlik, I.P.A., J. Comput. Aided Mol. Des., 7 (1993) 83.

45. Norinder U. (1995) The Alignment problem in 3D-QSAR: A combined approach using CATALYST and a 3D-QSAR technique, QSAR and Molecular Modelling: Concepts, Computational Tools and Biological Applica-

tions In Sanz, F. Giraldo, J., Manaut F. (Eds.), Prous Science Publishers, Barcelona, pp. 433–438.

46. Hoffmann, R.D. and Langer, T., Use of the CATALYST program as a new alignment tool for 3D-QSAR", QSAR and Molecular Modelling: Concepts, Computational Tools and Biological Applications, In Sanz, , Giraldo, F. and Manaut, J.F. (Eds.), Prous Science Publishers, Barcelona, 1995, pp. 466–469.

47. Langer, T. and Hoffmann, R.D., J. Chem. Inf. Comput. Sci., 38 (1998) 325.

48. Palomer, A., Pascual, J., Cabré, F., García, M.L. and Mauleón, D., J. Med. Chem., 43 (2000) 392.

49. Bureau, R., Daveu, C., Baglin, I., Sopkova-De Olivera Santos, J., Lancelot, J.-C. and Rault, S., J. Chem. Inf. Comput. Sci., 41 (2001) 815.

50. Golbraikh, A. and Tropsha, A., J. Mol. Graphics Model., 20 (2002) 269.

51. Wold S., Martens, H., Wold, H. (1983) In Ruhe, A., Agstrom B.K (Eds.), Springer Verlag, Heidelberg.

52. Wold, S., Technometrics, 20 (1978) 397.

53. Saxena Prathipati, A.K.P., SAR and QSAR Environ. Res., 14 (2003) 433.

54. Sprague, P.W., Automated chemical hypothesis generation and database searching with CATALYST, In Muller, K. (Ed) perspectives in Drug Discovery and Design. ESCOM:, Leiden, 1995, pp. 1–20.

55. Apex-3D version 1.4 user guide, Biosym MSI, San Diego, Sept. 1993.

56. Pandya, T., Pandey, S.K., Tiwari, M., Chaturvedi, S.C. and Saxena, A.K., Bioorg. Med. Chem., 9 (2001) 291.

57. Saxena, A.K., Pandey, S.K., Seth, P., Singh, M.P. and Dikshit Carpy, M. A., Bioorg. Med. Chem., 9 (2001) 2025.

58. Pandey, S.K., Naware, N.B., Trivedi, P. and Saxena, A.K., SAR and QSAR Envir. Res., 12 (2001) 547.

59. Babu, M.A., Shakya, N., Prathipati, P., Kaskhedikar, S.G. and Saxena, A.K., Bioorg. Med. Chem., 10 (2002) 4035.

60. Saxena, A.K., Pandey, S.K., Tripathi, R.C. and Raghubir., R, Bioorg. Med. Chem., 9 (2001) 1559.

61. Kashaw, S.K., Rathi, L., Mishra, P. and Saxena, A.K., Bioorg. Med. Chem. Lett., 13 (2003) 2481.

62. Rathi, L., Kashaw, S.K., Dixit, A, Pandey, G, Mishra, P. and Saxena, A.K., Bioorg. Med. Chem., (2004) in press.

63. Brooks, B.R., Bruccoleri, R.E., Olafson, B.D., States, D.J., Swaminathan, S. and Karplus, A.M., J. Comp. Chem., 4 (1983) 187.

64. Gundertofte, K., Liljefors, T., Norrby, P-O and Pattesson, I., J Comp Chem., 17 (1996) 429.

65. Bostrom, J., J. Comput. Aided Mol. Des., 12 (2001) 1137.

66. Smellie, A.S., Kahm, S.D. and Teig, S.L., J. Chem. Inf. Comput. Sci., 35 (1995) 285.

67. Smellie, A.S., Teig, S.L. and Kahm, S.D., J. Chem. Inf. Comput. Sci., 35 (1995) 295.

68. Greene, J., Kahn, S., Savoj, H., Sprague, P. and Teig, S., J. Chem. Inf. Comput Sci., 34 (1994) 1297.

69. Sutter, J., Guner, O., Hoffman, R., Li, H. and Waldman, M., Effect of Variable Weights and Tolerances on Predictive Model Generation, in Pharmacophore Perception, Development, and Use in Drug Design, O.F. Guner, Ed., International University Line, La Jolla, CA, 2000.

70. Dauber-Osguthorpe, P., Roberts, V.A., Osguthorpe, D.J., Wolff, J., Genest, M. and Hagler, A.T., Proteins: Struct. Funct Genet. 4 (1988) 31.

71. Hobza, P., Kabelac, M., Sponer, J., Mejzlik, P. and Vondrasek, J., J. Comp. Chem., 18 (2000) 1136.

72. Weyer, C. and de Souza, C.J, Drug Dev. Res., 51 (2000) 80.

73. de Souza, C.J., Hirshman, M.F. and Horton, E.S., Diabetes, 46 (1997) 1257.

74. Shih, T.L., Candelore, M.R., Cascieri, M.A., Chiu, S.H., Colwell, L.F Jr., Deng, L., Feeney, W.P., Forrest, M.J., Hom, G.J., MacIntyre, D.E., Miller, R.R., Stearns, R.A., Strader, C.D., Tota, L., Wyvratt, M.J., Fisher, M.H. and Weber, A.E., Bioorg Med. Chem. Lett., 9 (1999) 1251.

75. Parmee, E.R., Naylor, E.M., Perkins, L., Colandrea, V.J., Ok, H.O., Candelore, M.R., Cascieri, M.A., Deng, L., Feeney, W.P., Forrest, M.J., Hom, G.J., MacIntyre, D.E. , Miller, R.R., Stearns, R.A., Strader, C.D., Tota, L., Wyvratt, M.J., Fisher, M.H. and Weber, A.E., Bioorg. Med. Chem. Lett., 9 (1999) 749.

76. Dianippon Pharma Co. 1998. AJ-9677: β_3-adrenoceptor agonist. Pharmacological study report Ed. #1 (non-confidential information). Research and Development Headquarters.; Kawashima, H., Nomura, A., Ohue, M., Kato, H., Kuwajima, J., Furutani, Y., Hosoki, K., Diabetologia, 40 (1997) A374.

77. Hargrove, D.M., Dow, R.L., Martin, K.A., Nardone, N.A., Orena, S.J., Brodeur, A.M., Torchia, A.J., Kreutter, D.K., Yee, S. and Stevenson, R.W., Obes Res., 7 (1999) 72S.

78. Miller, J.W., Farid, N.A., Johnson, R.D., Smith, B.P. and Dananberg, J., Obes. Res., 7 (1999) 121S.

79. Lee, T.-L., Hsu, C.-T., Yen, S.-T., Lai, C.-W. and Cheng, J.-T., J. Auton. Nerv. Sys., 11 (1998) 86.

80. Blin, N., Camoin, L., Maigret, B. and Strosberg, A.D., Mol. Phar., 44 (1994) 1094–1104.